基于多时相遥感影像的浑善达克沙地沙漠化监测

刘海江[1,2], 周成虎[1,*], 程维明[1], 龙 恩[1], 李 锐[1,3]

(1. 中国科学院地理科学与资源研究所 资源与环境信息系统国家重点实验室, 北京 100101;
2. 中国科学院研究生院, 北京 100039; 3. 解放军信息工程大学, 郑州 450052)

摘要:沙漠化是浑善达克沙地面临的主要环境问题。为了揭示该地区沙漠化过程,特别是其最新状态,利用 1987 年和 2000 年的 Landsat TM/ETM$^+$及 2006 年的中巴资源卫星 CCD 数据,在地面考察资料及地理信息系统(GIS)的支持下,提取了固定沙地、半固定沙地、流动沙地、丘间草原及湿地 5 种地表覆被类型,建立了浑善达克沙地沙漠化数据库。

结果表明浑善达克沙地在过去 20a 里发生了沙漠化,但是可分为两个阶段。第一阶段从 1987 年到 2000 年,为沙漠化快速发展期,固定沙地面积显著减少,而半固定沙地和流动沙地则明显增加;第二阶段从 2000 年到 2006 年,为沙漠化缓减期。尽管发生了沙漠化,但固定沙地仍然是浑善达克沙地面积最大的类型。针对流动沙地的空间变化检测表明在过去 20a 里沙地恶化的面积远远大于逆转的面积,并且已经形成了几条流动沙带,这意味着浑善达克沙地沙漠化的遏制是一个长期的过程。

关键词:浑善达克沙地;沙漠化;中巴资源卫星;遥感;变化检测

文章编号:1000-0933(2008)02-0627-09 **中图分类号**:Q142, S157, S812 **文献标识码**:A

Monitoring sandy desertification of the Otindag Sandy Land based on multi-date remote sensing images

LIU Hai-Jiang[1,2], ZHOU Cheng-Hu[1,*], CHENG Wei-Ming[1], LONG En[1], LI Rui[1,3]

1 *Institute of Geographic Sciences and Natural Resources Research, China Academy of Sciences, State Key Laboratory of Resources and Environmental Information System, Beijing* 100101, *China*

2 *Graduate School of Chinese Academy of Sciences, Beijing* 100039, *China*

3 *Information Engineering University of People's Liberation Army, Zhengzhou* 450052, *China*

***Acta Ecologica Sinica*, 2008, 28(2): 0627 ~ 0635.**

Abstract: Sandy desertification is the main ecological problem the Otindag Sandy Land at present. In order to reveal the process of land degradation, especially the latest situation of sandy desertification, a method integrating remote sensing, Geographic Information System (GIS) and field survey was employed to build a sandy desertification dataset for analysis. Remote sensing images included the Landsat Thematic Mapper (TM) in 1987, the Enhanced Thematic Mapper plus (ETM$^+$) in 2000, and the Charge Coupled Device Camera (CCD) of China-Brazil Earth Resource Satellite (CBERS) in 2006. Five land-cover classes, including active sand dunes, fixed sand dunes, semi-fixed sand dunes, inter-dune grassland and wetlands, were identified.

Results showed that the Otindag Sandy Land has been suffering sandy desertification since 1987 with two different desertified stages. First stage from 1987 to 2000 is a serious sandy desertification period, characterized by the fixed sand

基金项目:国家自然科学基金资助(4040104)

收稿日期:2007-07-06; **修订日期**:2007-11-28

作者简介:刘海江(1978 ~), 男, 内蒙古呼和浩特市人, 博士生, 主要从事遥感、地理信息系统生态学应用研究. E-mail: liuhj@lreis.ac.cn

* 通讯作者 Corresponding author. E-mail: zhouch@lreis.ac.cn

Foundation item: The project was financially supported by National Natural Science Foundation of China (No. 4040104)

Received date: 2007-07-06; **Accepted date**: 2007-11-28

Biography: LIU Hai-Jiang, Ph. D. candidate, mainly engaged in RS and GIS application. E-mail: liuhj@lreis.ac.cn

dunes decreasing at a high speed, and the semi-fixed and active sand dunes increasing remarkably. The second stage spanned from 2000 to 2006 and the sandy desertification was weakened greatly. Although a large area of fixed sand dunes transformed to other types, it is still the dominant type in the Otindag region at 2006. Spatial change detection based on active sand dunes showed that the area of expansion is much larger than that of reversion in the past two decades, and that several active sand belts have been formed. It suggests that sandy desertification controlling of the Otindag Sandy Land will be a long-time task.

Key Words: Otindag Sandy Land; sandy desertification; CBERS; remote sensing; change detection

Sandy desertification is one of the main forms of land degradation in China, especially in northern China[1], which kept expanding since the 1950's and has exerted severe impacts on regional socio-economic development and environmental security[2]. Harsh physiographic conditions (sparse vegetation coverage, sandy soil, and water deficiency), irrational land-use practice and population augmentation are seen as the forces of triggering sandy desertification[3,4]. Therefore the sandy desertification assessment and monitoring are always concerned by researchers, the public, and policy-makers.

The Otindag Sandy Land, one of the four largest sandy lands in China, has suffered serious sandy desertification in the past decades[3,5,6]. The degraded land augmented 492 km^2/a during the 1950s to the middle of 1970s, 205 km^2/a from the middle of 1970s to the middle of 1990s, and 2015 km^2/a from the middle of 1990s to 2000[5]. This region has been thought as a source of sandy dust storm[7,8]. Therefore, it's very necessary to monitor sandy desertification of this region.

The major objective of this study is to assess sandy desertification process of the Otindag Sandy Land in the past decades. A method of integrating remote sensing, geographic information system (GIS), and field survey is employed to generate a sandy desertification dataset of this region. Then, change detection and land degradation process are performed based on the dataset. This project intends to provide useful information for sandy desertification controlling and environmental management of the Otindag area.

1 Study area

The Otindag Sandy Land (42°10′—43°50′N, 112°10′—116°30′E) is located in the southeastern part of Inner Mongolia[9] (Fig. 1), which is about 340 km long from east to west and 30—100 km in width. The elevation varies between 1400m and 1100m and the topography declines from southeast to northwest. The climate is temperate continental semi-arid type with strong wind and less precipitation in winter and in spring. Annual average precipitation, mainly occurring in summer and fall with some inter-annual fluctuation, is nearly 400mm in the southeastern part and below 200mm in the northwest[10,11]. The dominant vegetation is *Stipa grandis* and *Leymus chinensis* steppe. However, because of sandy substrate, the Otindag Sandy Land possesses a high biodiversity and spatial heterogeneity. The notable landscape is open forest steppe dominated by *Ulmus pumila*[12].

2 Data and methods

2.1 Data and pre-processing

Remotely sensed images used in this study include the Landsat5 Thematic Mapper (TM), the Landsat7 Enhanced Thematic Mapper plus (ETM^+), and the Charge Coupled

Device Camera (CCD) of China-Brazil Earth Resource Satellite (CBERS), which were acquired in 1987, 2000, and 2006 (Table 1). The ETM^+ images were acquired eventually in 1999, 2000, and 2001, hereafter named as the 2000 data. The CBERS was jointly developed by China and Brazil since 1988, which planned to launch a series of satellites used for resources and environmental monitoring. Two satellites (CBERS-1, 2) were launched in

October of 1999 (CBERS-1) and 2003 (CBERS-2) respectively. The CCD is one of the three sensors loaded on the CBERS, which has a nadir spatial resolution of 19.5 meters, swath width of 113 km, and five spectral bands including blue (0.45 − 0.52μm), green (0.52 − 0.59μm), red (0.63 − 0.69μm), near infrared (0.77 − 0.89μm), and panchromatic band (0.51 − 0.73μm). More information can be found at the website of the China Center for Resource Satellite Data and Applications (CRESDA) at http://www.cresda.com.cn/. All these data have been processed to level 2 by data supply agency, namely systematic geometric correction and radiometric calibration was performed. Here, they are geo-referenced to the Albers Equal-area Conic coordinate system using ground control points (GCP) based on 1:100000 scale topographic maps, and the root mean square error was less than one pixel.

Table 1　Characteristics of remotely sensed images used in this study

Scene's ID(Path-row) **Acquired time**(year-month-day) **Sensor type**

Scene's ID (Path-row)	Acquired time (year-month-day)	Sensor type
123-30	1987-09-10	TM
	2001-07-06	ETM$^+$
124-30	1987-07-31	TM
	2000-07-10	ETM$^+$
125-30	1987-10-27	TM
	1999-07-23	ETM$^+$
126-30	1987-06-27	TM
	1999-09-24	ETM$^+$
001-051,052,053	2006-09-06	CCD
002-051,052	2006-07-13	CCD
003-051,052	2006-08-31	CCD
004-051,052	2006-09-23	CCD
005-051,052	2006-07-30	CCD
006-051,052	2006-07-27	CCD

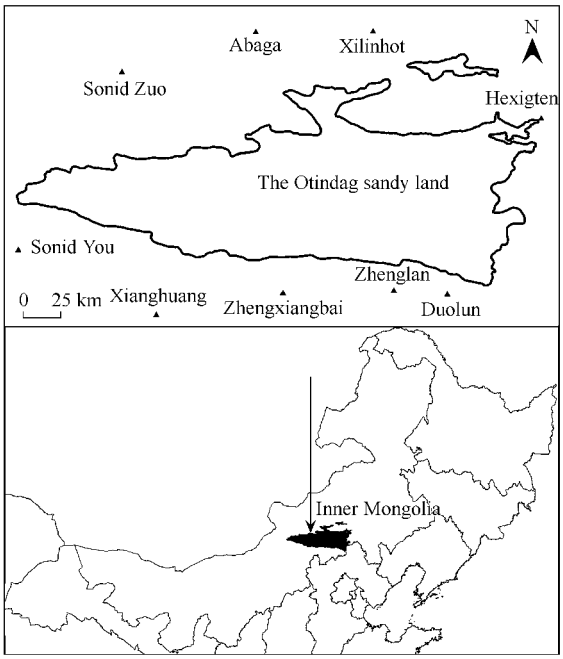

Fig. 1　Location of the Otindag Sandy Land

In order to remove or normalize the reflectance variation between images acquired at different time, relative radiometric correction was performed to yield radiometric normalized data in a common scale[13]. Here, the histogram normalization, a simpler and effective technique, was used to carry out the relative radiometric correction[14]. As for the Landsat images, the data of 2000 are used as master images to correct that in 1987. Whereas, the CCD data was calibrated among paths and the 003 path, which has the best quality through visual inspection, was used to match with the others. The near infrared, red and green bands were stacked into false-color image of different scenes in the same path and mosaicked them together, then path to path histogram normalization was performed.

2.2　Spectral transformation of Landsat images

Spectral transformation can reduce multi-spectral data volume with minimal information loss and generate a new image which loads main information of original data, which is an effective technique in improvement classification accuracy and change detection[16]. The Tasseled Cap transformation, also called as K-T transformation and originally applied to the Landsat Multispectral Scanner (MSS) data, is a principal component analysis technique, which transforms multi-spectral data linearly and creates three uncorrelated bands: Brightness (B), Greenness (G) and Wetness (W)[15-17]. The Tasseled Cap transformation is scene independent and has fixed coefficients, therefore, the multi-date TM and ETM$^+$ data can be transformed through this technique and the results are comparable across

dates. The BGW bands are directly related to specific physical attributes and can be easily interpreted. Brightness can be interpreted as change in total reflectance or albedo at the surface, and is driven mainly by soil reflectance variations; Greenness measures the contrast between visible bands and near infrared band and has a close correlation with vegetation coverage, just similar as vegetation index; Wetness is sensitive to soil and plant moisture[17]. After transformation, the BGW bands were combined into a new image.

2.3 Generating sandy desertification dataset

2.3.1 Class definition

Vegetation coverage is the most remarkable symbol of sandy desertification situation[3]. Several land cover types were identified according to vegetation coverage, meanwhile species composition and structure of plant community were also considered. They are active sand dunes, fixed sand dunes and semi-fixed sand dunes, which not only reflect ecological conditions that are important to environment management and resource utility but also are distinguishable in remote sensing images. Active sand dunes, the most severely degraded type, are dominated by psammophytes and annual pioneer plants with high surface reflectance and lower greenness on image, and vegetation coverage is less than 20%. Semi-fixed sand dunes, a transition type, have vegetation coverage during 20% to 50%, which are transformed from fixed sand dunes or active sand dunes. Fixed sand dunes hold dense vegetation with coverage more than 50% and a high biodiversity, which have high greenness and low brightness on image. In addition, two other classes, wetland and inter-dune grassland, are also identified. Inter-dune grassland, mainly distributed in the eastern part of the Otindag Sandy Land, occurs in flat, undulated plains between sand dunes and has high resistant to disturbance, which can be used as mowing pasture and be cultivated. Wetlands, including water body, swamp, and dense bushwood, are water source for livestock and shelters for wild animal. Characteristics of the five classes were determined by field survey and remote sensing images.

Field work was carried out in July of 2001 and August of 2006, and data of 121 and 209 sample sites were collected respectively. At each site, the structure and species composition of plant communities, vegetation projected coverage, and soil features were recorded, meanwhile the location was positioned by the portable Global Positioning System (GPS) receiver. These sample points covered the entire Otindag Sandy Land and were digitized onto the images according to their geographic position.

2.3.2 Supervised classification and dataset building

Training pixels were selected for each class on images, and the maximum likelihood classification was carried out in ERDAS IMAGINE8.7 to derive the thematic maps of 1987, 2000, and 2006. After post-classification process, the accuracy assessment was performed. The 2000's and 2006's classified map were assessed by field survey data, all the points were employed to evaluate classification accuracy, *i.e.* 121 points in 2000 and 209 points in 2006. Error matrix was derived and the overall accuracy reached 89.25% and 92.34% respectively. Because of no appropriate reference data available for assessment 1987's classified map, we used the classified map of 2000 as reference data to evaluate it. One hundred and fifty points were randomly selected, and the overall accuracy is 87.33%. This means that all the maps are acceptable[18].

The three classification maps were subset to the boundary of the Otindag Sandy Land which was delimited by expert in aeolian landform according to remotely sensed images in 2000, then these raster classified maps converted to vector format of ArcGIS. The patches of different classes in classified maps were represented as polygons in ArcGIS which were enclosed by a group lines connected each other. Visual inspection was conducted through superimposing the field survey points, remote sensing images and vector sandy desertification data together to correct some misclassified classes, then, sandy desertification dataset was built up (Fig.2).

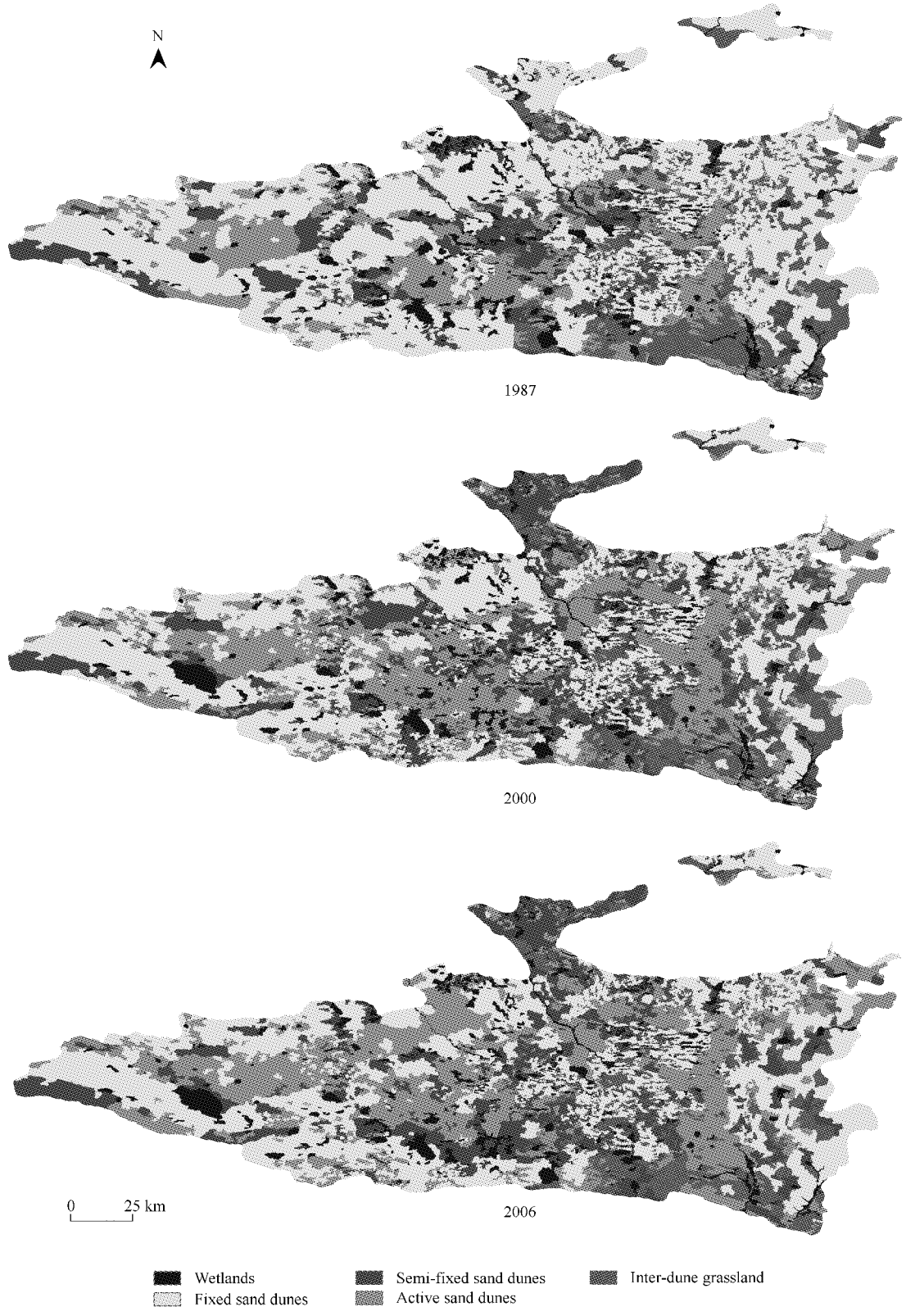

Fig. 2　Maps of sandy desertification in Otindag Sandy Land at 1987, 2000, and 2006

2.4　Change detection

In order to reveal sandy desertification process in Otindag area, change detection was carried out based on

active sand dunes in 1987, 2000 and 2006 because the active sand dunes can be used as an indicator of sandy desertification situation. At first, five classes were regrouped into active sand dunes and non-active sand dunes, then the dataset was converted into ArcGIS raster format GRID with binary values 0 (non-active sand dunes) and 1 (active sand dunes) coded. The pixel size is 30 meters. The binary GRID of 1987, 2000, and 2006 were combined to generate a new GRID with 2^3 different outcomes included 000, 010, 100, 110, 011, 001, 101, and 111 (Fig. 3). The figure of every outcome is arranged in time order, for example the 101 indicates that a pixel was active sand dunes in 1987, non-active sand dunes in 2000 and returned to active sand dunes in 2006. So, every outcome implied one kind of change trajectory of active sand dunes.

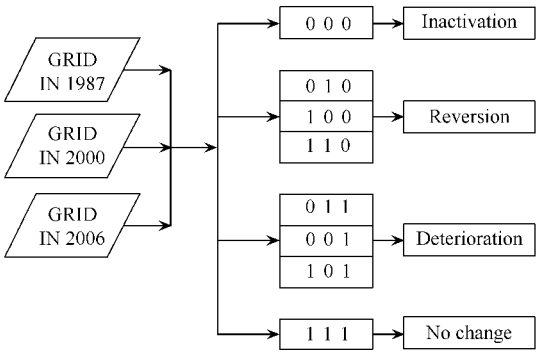

Fig. 3 Types of change detection

According to the change trajectory of active sand dunes, the eight outcomes were grouped into four classes named as inactivation, reversion, deterioration and no change. The inactivation, including 000, means that pixels kept non-active sand dunes from 1987 to 2006. Reversion type, including 010, 100, and 110, implies that pixels were active sand dunes at 1987 or 2000, and converted to non-active sand dunes in 2006; Deterioration type, containing 011, 001, and 101, is just opposite to the reversion, which means pixels belonged to non-active sand dunes at 1987 or 2000, and transformed to active sand dunes at 2006; No change class, including 111, means that pixels retained active sand dunes during 1987 to 2006.

3 Results

3.1 Sandy desertification processes

Remarkable ecological change occurred in the Otindag Sandy Land in the past decades. During 1987 to 2006 the fixed sand dunes, which covered half area (14,570.93 km^2, 50.25%) in 1987, sharply shrank to 10,608.96 km^2(36.6%) in 2000 with a decreased rate of 304.77 km^2/a. The semi-fixed sand dunes, however, increased from 3,405.41km^2(11.70%) in 1987 to 4,911.13 km^2 (16.94%) in 2000 with a growth rate of 115.82 km^2/a. The active sand dunes, following the same trend with the semi-fixed sand dunes, increased to 8090.70km^2 (27.91%) in 2000 with an change rate of 201.67 km^2/a. The inter-dune grassland decreased at a rate of 22.20km^2/a, whereas wetlands increased slowly with 9.47 km^2/a (Table 2, Fig. 4).

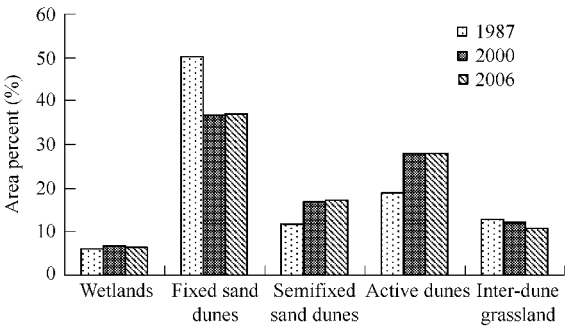

Fig. 4 Area percent of five land cover types in 1987, 2000, and 2006 in Otindag area

In contrast, there was some differences in land degradation process from 2000 to 2006 with the first period. The noticeable change is fixed sand dunes increasing with a rate of 30.31 km^2/a. The semi-fixed sand dunes and active sand dunes remained augmentation, but the increased magnitude was sharply declined. However, the inter-dune grassland reduced at a higher speed. Wetlands decreased with a speed of 7.18 km^2/a. Although the decrease in area is significant, the fixed sand dunes remained the largest area in Otindag Sandy Land in 2006 (Table 2).

We can conclude from the results that the sandy desertification process of the Otindag Sandy Land can be divided into two different stages. First stage, from 1987 to 2000, was characterized by the land degradation with a

high speed; whereas the second stage, during 2000 to 2006, the ecological deterioration presented a notable alleviation.

Table 2　Change rate of five land cover classes during 1987 to 2006 in Otindag area land cover types

Land cover types	Area(km^2)			Change rate(km^2/a)(+ Gain, - Loss)	
	1987	2000	2006	1987 ~ 2000	2000 ~ 2006
Fixed sand dunes	14570.93	10608.96	10790.84	-304.77	+30.31
Semi-fixed sand dunes	3405.41	4911.13	5039.75	+115.82	+21.44
Active sand dunes	5468.99	8090.70	8160.94	+201.67	+11.7
Inter-dune grassland	3761.75	3473.23	3135.59	-22.20	-56.27
Wetlands	1784.76	1907.86	1864.78	+9.47	-7.18

3.2　Spatial change detection

Change detection could reveal the dynamic of sandy desertification in spatial. As shown in Fig. 5, the four classes presented different patterns. Deterioration mainly occurred at periphery of no change class, namely emergence of new active sand dunes was based on the old ones which kept active in the past two decades. Therefore, the patches of deterioration class and no change class were combined and formed several active sand belts (Fig. 5). Reversion class mainly covered in central-south part of Otindag area.

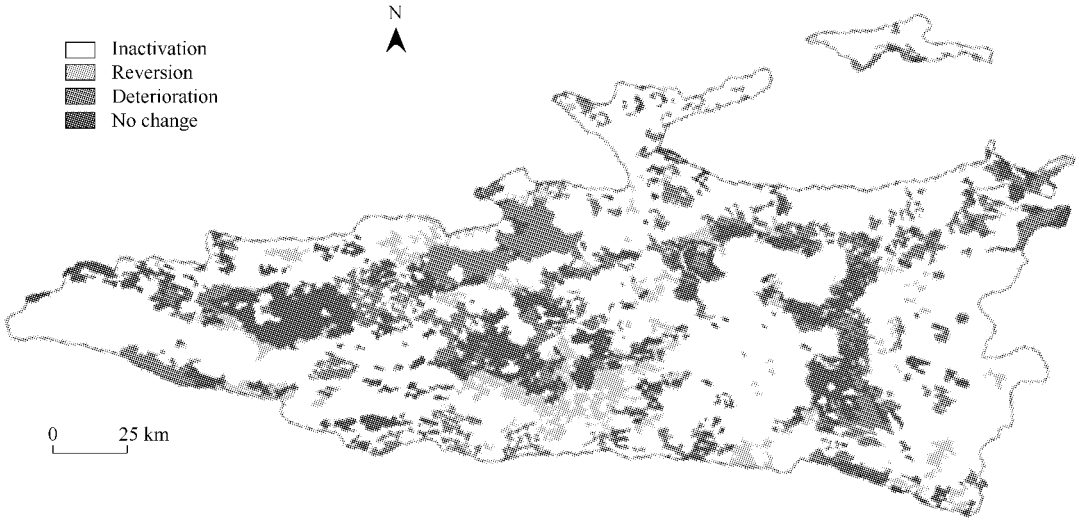

Fig. 5　Change detection of active sand dunes during 1987 to 2006 in Otindag area

Land degradation is the main ecological process in Otindag area in the past two decades. Pixels of deterioration (4579057) were almost twice more than that of reversion (2303715). And no change (4484457) was also nearly twice larger than reversion. However, inactivation was still the dominated class which had the most pixels (20832938) among the four types (Table 3).

Table 3　Pixel number of four change detection classes

Inactivation	Reversion	Deterioration	No change
20832938	2303715	4579057	4484457

4　Discussion and conclusion

The Otindag Sandy Land became a hot spot because of the 2000's widespread sand storms. In this research, we employed the temporal remote sensing images to reveal the sandy desertification process in this region, especially the latest situation of sandy desertification.

Sandy desertification had occurred in the Otindag Sandy Land in the past two decades from 1987 to 2006. The

fixed sand dunes shrank, semi-fixed and active sand dunes increased remarkably, meanwhile, the inter-dune grassland and wetlands were also decreased (Table2, Fig. 4,5). Two different sandy desertification stages can be identified. The first stage, from 1987 to 2000, land degradation proceeded at a higher speed, whereas during 2000 to 2006, sandy desertification was greatly alleviated. Although severe land degradation occurred, the fixed sand dunes still dominated in Ointdag area in 2006. The spatial change detection showed that area of deterioration was much larger than that of reversion, and that several active sand belts had been formed (Table3, Fig. 5).

Ecological deterioration of this region is mainly a human-induced process, and the climate had not notable changes only with normal fluctuation[19-21]. In the past two decades, this region experienced rapid population increase. Life demand of local people caused overgrazing and reclamation on grassland for improve income. Meanwhile, no adequate attention was paid to protecting and restoring vegetation. In consequence, it led to degradation of natural vegetation and triggered sandy desertification.

Policies play an important role in controlling sandy desertification[22]. The alleviation of sandy desertification during 2000 to 2006 mainly resulted from a series of ecological restoration projects. In 2000, a national-wide ecological restoration project, named as the Grain-for-Green Project, was launched and regulations were enacted by the central government. This project aims to reduce the cropland which is not suitable for cultivation so as to restore natural vegetation. The ultimate goal is to attain sustainable development of society, economy and environment. In Otindag area, a series of measures, aimed at weakening the disturbance and increasing the coverage of natural vegetation, were taken by local governments to control further ecological degradation, which included grazing prohibition, plantation of high yield forage grasses, aerial seeding by plane, and adjustment of socio-economic structure. After several years' practice, the sandy desertification was greatly alleviated. From this research, we can suggest affirmatively that these measures were indeed effective in controlling land degradation, however, because of long time needed in restoration of damaged sandy ecosystem, the policies, made by decision-makers, be valid in a longer time span.

References:

[1] Wang T, Zhu Z D. Studies on the sandy desertification in China. Chin. J. Eco-agri., 2001, 9(2): 7-12.

[2] Wang T, Chen G T, Zhao H L, *et al*. Research progress on aeolian desertification process and controlling in north of China. J. Desert Res., 2006, 26(4): 507-516.

[3] Zhu Z D, Chen G T. Sandy desertification in China. Beijing: Science Press, 1994. 20-33.

[4] Chen Y F, Tang H P. Desertification in north China: background, anthropogenic impacts and failures in combating it. Land Degrad. Develop., 2005, 16: 367-376.

[5] Liu S L, Wang T. Primary study on sandy desertification in Otindag Sandy Land and its surrounding regions. J. Soil Water Conserv., 2004, 18(5): 99-103.

[6] Fan J Y, Ding G D, Guan B Y, *et al*. Monitoring remote sensing of dynamic change of vegetation coverage in Zhenglan Banner. Sci. Soil Water Conserv., 2005, 3(4): 54-59.

[7] Wang T, Chen G T, Qian Z G, *et al*. The situation of dust storms and its strategy in north China. Bull. Chin. Acad. Sci., 2001, 5: 343-348.

[8] Liu H Y, Tian Y H, Ding D. Contributions of different land cover types in Otindag Sandy Land and Bsshang region of Hebei Province to the material source of sand stormy weather in Beijing. Chin. Sci. Bull., 2003, 48(11): 1853-1856.

[9] Zhu Z D, Wu Z, Liu S. The generality of deserts in China. Beijing: Science Press, 1980. 80-107.

[10] Wang W H. Climate of Inner Mongolia. Beijing: China Meteorological Press, 1990. 183-188.

[11] Bai M L, Hao R Q, Di R Q, *et al*. Assessment of climatic variation impact on desertification of Otindag Sandland. Climatic Environ. Res., 2006, 11(2): 215-220.

[12] Guo K, Liu H J. A comparative researchs on the development of elm seedlings in four habitats in the Hunshandak Sandland, Inner Mongolia. Acta Ecologica Sinica, 2004, 24(9): 2024-2028.

[13] Paolini L, Grings F, Sobrino JA, *et al*. Radiometric correction effects in Landsat multi-date/multi-sensor change detection studies. Int. J. Remote Sens., 2006, 27: 685 -704.

[14] Ding L X, Zhou B, Wang R C. Comparison of five relative radiometric normalization techniques for remote sensing monitoring. J. Zhejiang Uni. (Agric. Life Sci.), 2005, 31(3): 269 -276.

[15] Zhao Y S. Principles and methods in remote sensing application and analysis. Beijing: Science Press, 2003, 188 -190.

[16] Seto K C, Woodcock C E, Song C, *et al*. Monitoring land-use change in the Pearl River Delta using Landsat TM. Int. J. Remote Sens., 2002, 23: 1985 -2004.

[17] Masoud A A, Koike K. Arid land salinization detected by remotely-sensed landcover changes: A case study in the Siwa region, NW Egypt. J. Arid Environ., 2006, 66: 151 -167.

[18] Congalton R G, Green K. Assessing the accuracy of remotely sensed data: principles and practices. Lewis Publishers: Boca Raton, London, New York, Washington, D.C.. 1999. 45 -55.

[19] Li Q F, Hu C Y, Wang M J. Analysis on the causes of eco-environmental deterioration in Hunshandake Sandy land region and countermeasures. J. Arid Land Resour. Environ., 2001, 15(3): 9 -16.

[20] Zheng Y R, Xie Z X, Robert C, *et al*. Did climate drive ecosystem change and induce desertification in Otindag Sandy Land, China over the past 40 years? J. Arid Environ., 2006, 64: 523 -541.

[21] Liu S L, Wang T. Characteristic of climatic change in the Otindag Sandy Land region. J. Desert Res., 2005, 25(4): 557 -562.

[22] Oñate J J, Peco B. Policy impact on desertification: stakeholders' perception in southeast Spain. Land Use Pol., 2005, 22: 103 -114.

参考文献:

[1] 王涛, 朱震达. 中国沙漠化研究. 中国生态农业学报, 2001, 9(2): 7~12.

[2] 王涛, 陈广庭, 赵哈林,等. 中国北方沙漠化过程及其防治研究的新进展. 中国沙漠, 2006, 26(4): 507~516.

[3] 朱震达, 陈广庭. 中国土地沙质荒漠化. 北京:科学出版社, 1994. 20~33.

[5] 刘树林, 王涛. 浑善达克沙地地区土地沙漠化初步研究. 水土保持科学, 2004, 18(5): 99~103.

[6] 范建友,丁国栋,关博源,等. 正兰旗植被覆盖动态变化的遥感监测. 中国水土保持科学, 2005, 3(4): 54~59.

[7] 王涛,陈广庭,钱正安,等. 中国北方沙尘暴现状及对策. 中国科学院院刊, 2001, 5: 343~348.

[8] 刘鸿雁, 田育红, 丁登. 内蒙古浑善达克沙地和河北坝上地区不同地表覆盖类型对北京沙尘天气物源的贡献. 科学通报, 2003, 48(11): 1853~1856.

[9] 朱震达, 吴正, 刘恕. 中国沙漠概论. 北京:科学出版社, 1980. 80~107.

[10] 王文辉. 内蒙古气候. 北京:中国气象出版社, 1990. 183~188.

[11] 白美兰, 郝润全, 邸瑞琦, 等. 气候变化对浑善达克沙地沙漠化影响的评估. 气候与环境研究, 2006, 11(2): 215~220.

[12] 郭柯, 刘海江. 浑善达克沙地四种生境中榆树天然更新幼苗发育的比较. 生态学, 2004, 24(9): 2024~2028.

[14] 丁丽霞, 周斌, 王人潮. 遥感监测中5种相对辐射校正方法研究. 浙江大学学报(农业与生命科学版), 2005, 31(3): 269~276.

[15] 赵英时. 遥感应用分析原理与方法. 北京: 科学出版社, 2003, 188~190.

[19] 李青丰, 胡春元, 王明玖. 浑善达克地区生态环境劣化原因分析及治理对策. 干旱区资源与环境, 2001, 15(3): 9~16.

[21] 刘树林, 王涛. 浑善达克沙地地区的气候变化特征. 中国沙漠, 2005, 25(4): 557~562.